

OPTIMIZING HIGH ASPECT RATIO COMPOSITE WINGS THROUGH GEOMETRICALLY NONLINEAR AEROELASTIC TAILORING

Touraj Farsadi^{1,2}, Majid Ahmadi² and Hamed Haddad Khodaparast²

¹ Swansea University, Aerospace Engineering Department, UK

² Adana Alparslan Turkes Science and Technology University, Aerospace Engineering Department, Türkiye

Keywords: High aspect ratio wing, Composite material, Aeroelastic tailoring, Multi-disciplinary Design Optimization, Numerical Simulation

Abstract: This paper introduces an approach to optimize high aspect ratio composite aircraft wings, aiming to enhance performance. Leveraging materials like carbon fiber and efficient manufacturing techniques, these wings promise lighter aircraft and reduced fuel consumption. However, achieving these benefits requires addressing structural and aeroelastic constraints. The proposed method, aeroelastically tailored Multi-objective, Multi-disciplinary Design Optimization (MMDO), integrates numerical techniques, including Finite Element (FE) modeling and hybrid Particle Swarm Optimization (PSO) and Genetic Algorithm (GA) optimization methods, within the Nonlinear Aeroelastic Simulation Software (NAS²). The paper notably introduces a two-way coupling method for nonlinear static aeroelastic analysis, ensuring seamless integration between aerodynamic and structural solvers. This integration takes place within the NAS² software framework, purpose-built for solving aeroelastic problems. Additionally, the Reduced Order Method (ROM) is employed to solve dynamic aeroelastic problems, including flutter and gust analysis. NAS² serves as a reliable and efficient platform for coupling and automating diverse simulation codes, typically encompassing aerodynamics and structural mechanics, thus enabling precise simulation of the interaction between aerodynamics and structures. The present work considers critical factors such as buckling, static deformations, composite failure criteria, flutter and gust responses in optimizing highly flexible composite wings while addressing geometrically nonlinear deformation constraints.

1. INTRODUCTION

Optimizing weight has a direct impact on the structural integrity and aeroelastic performance of an aircraft. Reducing the weight of the wing decreases the strain on the structure, optimizes the fuel efficiency, and improves the overall performance. Striking the correct balance between structural, aeroelastic, and material requirements is crucial in designing high aspect ratio wings. These wings experience significant bending and torsional forces, requiring careful design to avoid failure. Therefore, it is crucial to combine weight optimization with aerostructural analysis in order to guarantee both strength and lightness. Extensive research has focused on using composite materials to adjust the aeroelastic properties of aircraft wings in order to improve the aeroelastic performance of the wing structure [1-5]. The sizing of the structure is mostly determined by static maneuver load scenarios in several studies [6-8].

Mitrotta et al. [9] proposed a novel design approach that utilizes Proteus, OptiBLESS, and MSC Nastran for aeroelastic tailoring, optimization, and analysis, respectively. By utilizing the MDO

method in many investigations [10-13], the researchers concentrated on decreasing the weight of the wing in both static and dynamic aeroelastic circumstances. Benaouali and Kachel [14] automated the numerical simulation to optimize aircraft wings, resulting in an 8.9% increase in range by taking into account design elements. Silva et al. [15] conducted an optimization study on composite wings, taking into account variables such as strength, buckling, and flutter. Saporito et al. [16] created a framework that combines dynamic aeroelastic constraints to optimize the wings of aircraft during the initial stages of conceptual design. Rajpal et al. [17] underlined the necessity of a comprehensive strategy in optimizing wing structure by considering aerodynamic loads. Kilimtzidis and Kostopoulos [18] developed a numerical algorithm to determine the most efficient arrangement of high aspect ratio composite wings, taking into account static aeroelasticity. The German Aerospace Center (DLR) conducted a focused endeavor to optimize, manufacture, and test a wing with a typical cross-section that was optimized to be aeroelastically employing composite materials [19,20]. These investigations involve the production of the wing utilizing load-carrying skins that are packed with foam. The foam is used to prevent buckling by providing resistance. The omission of ribs and spars from the wing is a deliberate choice made to streamline the production process. Meddaikar et. al. [20] conducted a study on aeroelastic tailoring in composite wing design to achieve optimal stiffness. The wind tunnel experiments have verified the design's validity, demonstrating a strong correlation with the simulations. The study provides a comprehensive analysis of the optimization framework, wing manufacturing process, and experimental setup. Rajpal et al. [21] successfully validated a numerical design approach for improving composite wings subjected to gust and fatigue loads, confirming its efficacy. They utilized an analytical fatigue model instead of traditional approaches to improve precision and take advantage of the capabilities of composite materials. A rectangular composite wing is developed, constructed, and tested in the wind tunnel.

This work introduces an MDO method that aims to fill the existing gaps by specifically considering important variables such as length and thickness of the skin regions, and location of the ribs. The objective is to enhance performance by addressing issues related to buckling, deformations, stress limitations, and composite failure. The study provides benchmark data for the optimization of high aspect ratio composite wings. It also uses NAS² software [22-24], which is used for designing composite aircraft structures.

2 GENERAL MDO FRAMEWORK

This study utilizes the Particle Swarm Optimization (PSO) and Genetic Algorithm (GA) techniques to optimize variables associated with the arrangement, order, fiber angle, and spanwise division areas of the wing's composite structures. In this hybrid approach, the GA, an evolutionary heuristic algorithm, is first executed with an acceptable population size and number of generations to explore the global search space and find a near-optimal solution. This near-optimal solution is then used as the initial condition for the PSO algorithm, which simulates the social behavior of particles in a swarm to quickly and efficiently refine the solution in the local search space. By leveraging the global search capability of GA and the local search efficiency of PSO, this hybrid method can effectively reduce computational costs while achieving more accurate optimization results. Particle Swarm Optimization (PSO) offers several advantages, including its ease of implementation, efficiency in converging to good solutions quickly, flexibility to handle various optimization problems, independence from gradient information, ability to search for global

optima, robustness to parameter variations, and scalability to problems of different sizes and dimensions.

The hybrid algorithm is specifically designed to navigate within specified design constraints, taking into account various factors such as minimum safety factors, aeroelastic stability (including flutter and divergence speeds), gust loading, fabricated method, and the prevention of primary and secondary (shear) buckling and composite failure. The primary objective of the optimization procedure is to minimize the weight of the wing while simultaneously optimizing the unit twist factor.

This study examines the possibility of torsion-bending coupling in the composite wing by calculating the unit twist factor, which is obtained by dividing the torsion angle by the vertical deflection at the wing tip. The unit twist factor, offers insight into how much torsional deformation a wing undergoes relative to its flapwise bending deformation under aerodynamic loads. This factor impacts the wing's critical flutter speed, with higher unit twist factor values indicating greater torsional stiffness relative to bending stiffness and consequently higher flutter speeds. By focusing on optimizing unit twist factor, designers indirectly enhance flutter and divergence speeds, thus improving the wing's aeroelastic performance and stability. Therefore, considering both weight and the unit twist factor as objectives in composite wing optimization is both reasonable and often necessary for achieving an optimal design.

Figure 1 visually represents the steps and outcomes of the hybrid algorithm, showing the Design Structure Matrix (DSM) of the MDO in two level. At the first level of optimization, structural and composite analysis is performed, and the inner loop (level #1) must converge before the execution of the outer loop (level #2), which specifically addresses the dynamic aeroelastic criteria. At the outer loop of optimization, the analysis includes gust analysis, aeroelasticity, and structural dynamics. The optimization matrix undergoes an initial linear execution in the inner loop to establish approximate parameter limits, followed by a geometrical nonlinear execution. This entire process showcases the outcomes achieved through the PSO algorithm.

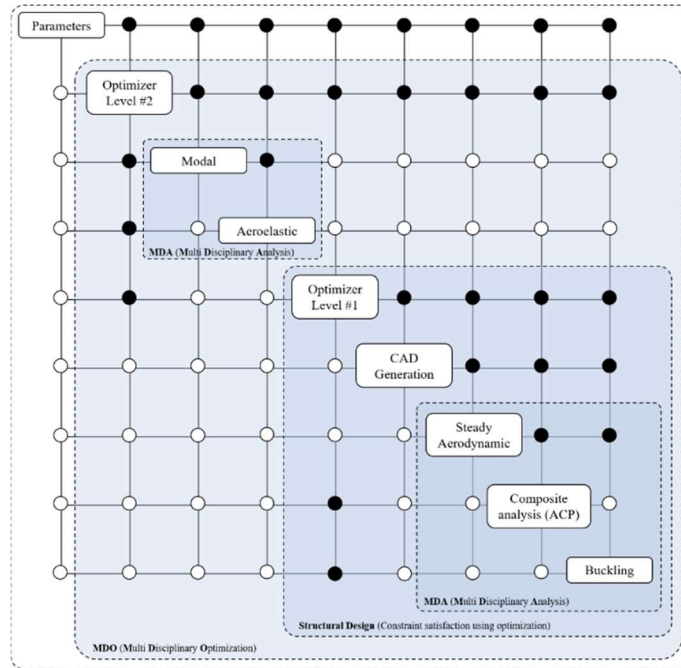


Figure 1. Design structure matrix (DSM) of the MDO.

Table 1 provides a summary of the MDO problem, which involves designing a wing that is both lightweight and flexible. The goal is to 1) minimize the weight of the wing while 2) maximizing its unit twist factor. Creating several laminates by splitting the upper and lower skins into regions along the span of the wing. The optimization procedure specifically targets the laminates in both the upper and lower skins. The optimization process aims to minimize the combined function $f(\mathbf{x})$, which represents the balance between reducing wing weight and maximizing the unit twist factor. The design variables (\mathbf{x}) consist of characteristics such as the lengths of regions for the top and lower skins, the number of layers for each skin, fiber angles, and rib placements. The optimization issue is shaped by constraints relating to buckling, static strength, composite failure, and aeroelastic instability.

Table 1. Optimization problem.

Objectives: Minimize the combined objective function $f(\mathbf{x})$ representing the trade-off between minimizing the wing weight and maximizing the unit twist factor:

$$f(\mathbf{x}) = \text{Wing Weight}(\mathbf{x}) - \lambda \times \text{Unit Twist Factor}(\mathbf{x})$$

where \mathbf{x} is the vector of design variables, and λ is a weight factor.

Variables: Design variables (\mathbf{x}):

Length of regions for the upper skin, L_i^U

Length of regions for the lower skin, L_i^L

Number of layers for the upper skin, N_i^U

Number of layers for the lower skin, N_i^L

Number of layers for the spar, N^S

Fiber angle for the upper skin, θ^U

Fiber angle for the lower skin, θ^L

Fiber angle for the spar, θ^S

Rib positions, pos^R

Constraints: The optimization problem is subject to the following constraints:

Load Multiplier: Buckling(\mathbf{x}),

Inverse Reserve Factor: Static Strength(x) and Composite Failure(x)
Flutter and Divergence: Aeroelastic Instability(x)
Manufacturability: See Figure 2

$$\theta_{max} = \tan^{-1} \left(\frac{-L^2b - c\sqrt{L^2(L^2 - b^2 + c^2)}}{(-bc + L\sqrt{L^2(L^2 - b^2 + c^2)})} \right)$$

Load Cases: The optimization considers three load cases:

Static Load (Function of *flight speed (U)* and *AOA (α)*)

Dynamic Load (Function of *flight speed (U)* and *AOA (α)*)

Gust Load (Function of *gust frequencies (F)* and *gust ratio (WG)*)



Figure 2. Ply angle and section length, where, the fiber fabric width is b , the ply lamina width is c and each lamina's length is L .

3 DESIGN FRAMEWORK

3.1 Structural analysis

Finite Element Method (FEM) is utilized to thoroughly examine the composite wing structure. This analysis incorporates primary and secondary buckling equations, taking into account the structural complexities, material characteristics, and loading circumstances. FEM utilizes numerical simulations to accurately determine critical loads and buckling modes, offering a comprehensive insight into the structural behavior of the wing.

The evaluation of the durability of the composite wing requires the implementation of the Tsai-Wu failure principle, the derivation of the stress state within the plane using FEM, and the calculation of strength ratios based on the stress components within the plane. To investigate out-of-plane failure, it is necessary to detect delamination events using a quadratic stress criterion and construct cohesive behavior between adjacent layers based on the surface [25]. In the context of safety analysis, the Inverse Reserve Factor (IRF) serves as an additional statistic to the Safety Factor (SF). The Safety Factor measures the margin to failure by multiplying the applied load, whereas the Inverse Reliability Factor (IRF) represents the failure load as the applied load divided by IRF. A Safety Factor more than one indicates a surplus of safety, meaning there is a positive margin before failure. Conversely, an IRF greater than one suggests a possibility of failure. The formula for the IRF is mathematically expressed as the reciprocal of the Safety Factor ($IRF = 1/SF$). Reserve factors have critical values ranging from zero to one, whereas non-critical values extend from one to infinity. The examination of the composite structure's Safety Margins ($SM = SF - 1$) takes into account several parameters, including fiber failure, matrix failure, in-plane shear failure, out-of-plane shear failure, delamination, and the Tsai-Wu factor. This comprehensive

approach ensures a thorough assessment of the safety margins. The focus on non-critical values, whether shown quantitatively or visually through contour plots, underscores their importance relative to crucial values.

3.2 Aeroelastic analysis

Two-way coupling is used to solve the present “geometrically nonlinear Static aeroelastic problem”, where the aerodynamic and structural solvers are integrated and exchange information continuously or at very short intervals. In two-way coupling, the aerodynamic and structural responses influence each other significantly and are updated iteratively until a converged solution is reached. The flowchart provided in Figure 3 outlines a sophisticated computational approach known as two-way coupling for static aeroelastic analysis. This method is pivotal for the detailed study of nonlinear aeroelasticity of high aspect ratio wing where the interactions between the structural dynamics and the inflow aerodynamics are both critical for the aerostructure's performance. The aeroelastic analysis discussed here involves iterative steps within a single time-step of a simulation, demanding convergence in both the aerodynamic and structure fields. In a two-way aeroelastic coupling method, lookup tables serve as intermediary repositories storing pre-computed aerodynamic coefficients or forces correlated with various structural deformations and flow conditions. By organizing aerodynamic and structural responses into lookup tables and employing interpolation techniques, the method ensures consistent coupling between the two domains, enabling accurate predictions of the wing's aeroelastic behavior while enhancing computational efficiency. This iterative process of interpolation within lookup tables continues until convergence is reached, iteratively refining the aerodynamic and structural solutions until they align, making the approach valuable for real-time simulations and design optimization studies. In addition, The flowchart depicted in Figure 3 offers a thorough representation of the “linear Dynamic aeroelastic solution” through Reduced Order Method (ROM).

The optimization flowchart consists of two main loops: an inner loop, known as "Constraint satisfaction using optimization," which aims to meet the static structural constraints through optimization, and an outer loop that verifies the dynamic structural constraints, specifically aeroelastic stability and gust response. After obtaining the wing's geometrical shape from the optimization process, a nonlinear static aeroelastic analysis is performed to determine the important static large deflections. This analysis captures the static equilibrium point once the iterative process has converged. The aerodynamic loads are recalculated for each deformed shape of the structure until convergence is reached. A post-convergence check is performed to verify compliance with optimization requirements for buckling and static restrictions. The optimizer will adjust the bounds of the inputs and iterate through the loop until all constraints are met, in the case of an unsatisfied constraint. After obtaining the static equilibrium point from the nonlinear static aeroelastic analysis, a flutter analysis is next conducted using a ROM. The purpose of modal analysis is to obtain the mode shapes and natural frequencies. The initial modes are then used in the ROM for flutter analysis until convergence is achieved. Subsequently, the P-k approach is utilized to create aeroelastic frequency and damping diagrams, which offer valuable information regarding the speed at which flutter occurs, the frequency of flutter, and the specific modes that contribute to instability. Once the instability speed falls within the allowed range, the optimization loop concludes.

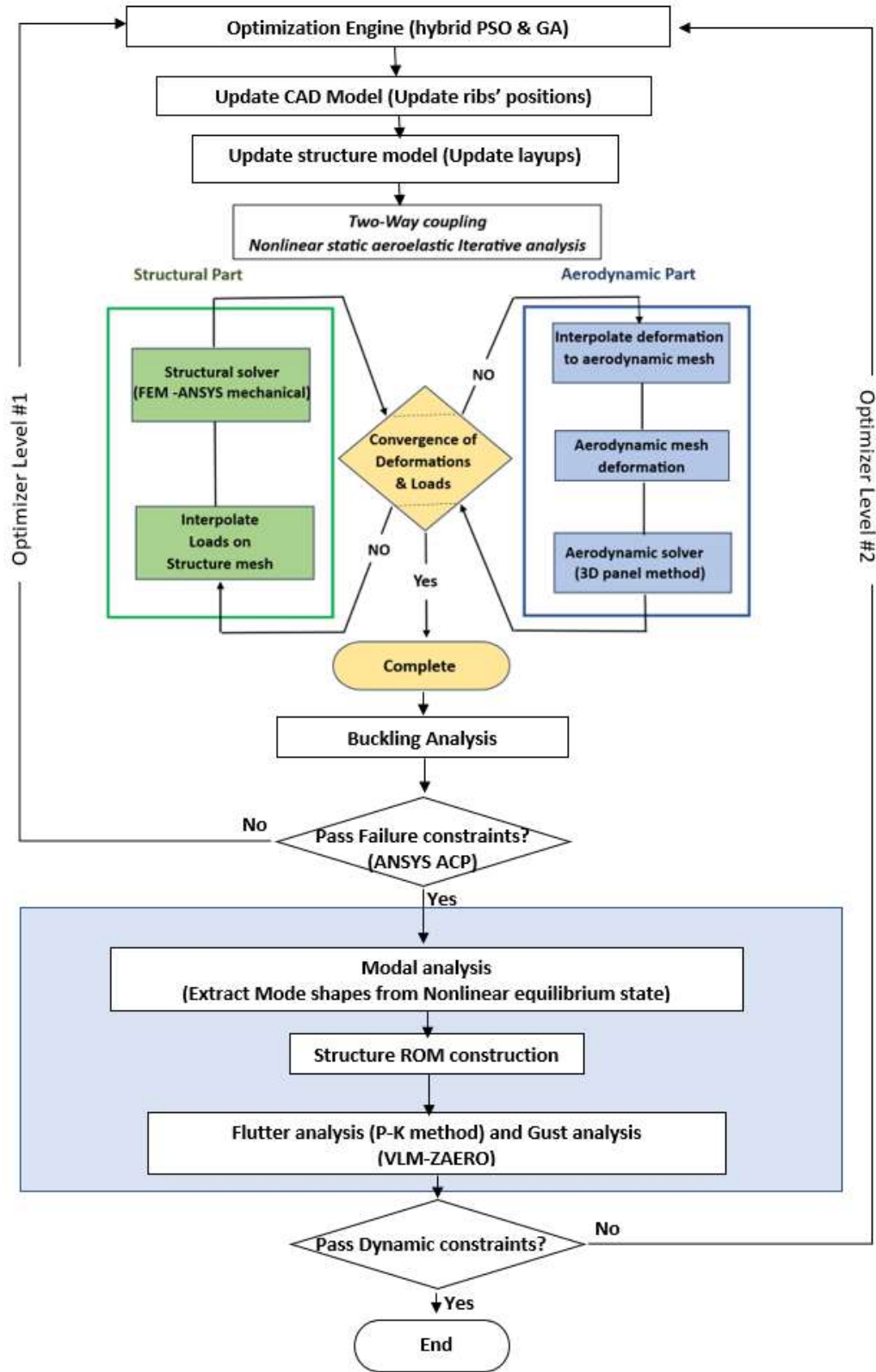


Figure 3 Aeroelastic solution and optimization procedure.

The two-way coupling technique for large deflection static aeroelastic analysis followed by modal analysis from the resulting nonlinear static state to perform flutter and gust analysis with a ROM leverages the strengths of each method. This hybrid approach effectively captures detailed static deformation and dynamic responses.

Combining high-fidelity static aeroelastic analysis with a ROM for dynamic analysis balances accuracy and computational efficiency, capturing complex deformation in the static analysis while enabling rapid dynamic simulations. The large deflection static analysis effectively captures nonlinear structural behavior and aeroelastic interactions, with modal analysis around the deformed state ensuring the ROM includes these nonlinear effects in the dynamic response. Additionally, the ROM's adaptability to various gust profiles and dynamic loading conditions offers flexibility in aeroelastic analysis. Using two-way coupling for the static analysis optimizes computational resources, with the less demanding ROM efficiently handling the dynamic simulations.

4 CASE STUDY - WING MODEL

The proposed method is used to optimize a composite UAV wing. The composite rectangular wing has a half span of 1.25 meters. The wingspan is chosen to ensure it fits within the test section for future wind tunnel experiments. The spar is positioned at a key location, specifically at 25% chord, which enhances the overall structural strength. The wing's shape is well-balanced, with a high aspect ratio of 14 and a taper ratio of 1. The NACA 0010 airfoil is utilized for the composite wing because to its favorable aerodynamic characteristics. The purpose of incorporating these design aspects and criteria is to enhance the overall performance and functionality of the composite wing seen in Figure 4, particularly in various aeroelastic and structural situations. In Figure 4, the lengths along the span in the upper skin are denoted as L_1^U, L_2^U and L_3^U , while in the lower skin, they are represented as L_1^L, L_2^L and L_3^L .

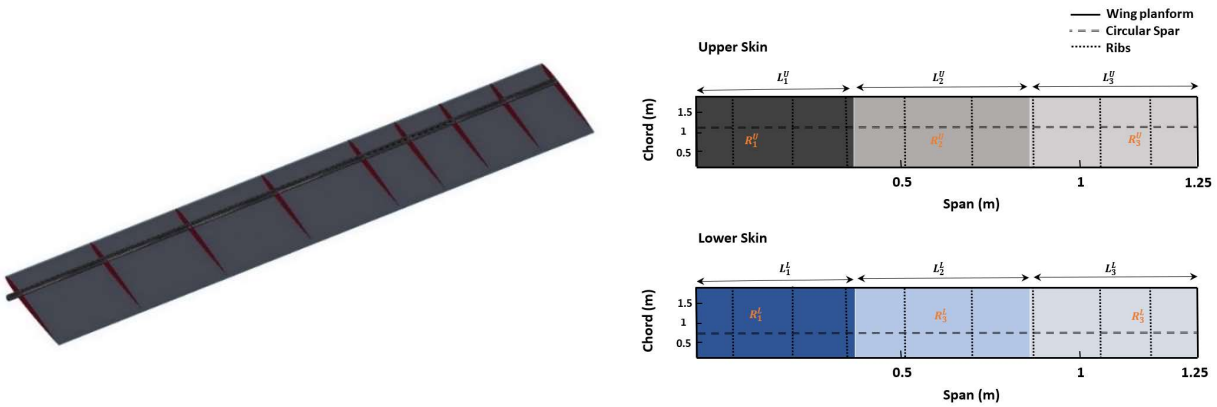


Figure 4. Graphical representation of baseline wing configuration as a case study. The design regions are indicated by different colors in the upper and lower skins.

In this study, a circular tube spar is used in the composite wing. The efficiency of a circular tube spar in a UAV high aspect ratio wing is a multifaceted consideration, encompassing factors such as weight-to-strength ratio, stiffness, manufacturing simplicity, cost-effectiveness, aerodynamic

performance, structural integration, fatigue resistance, safety, and redundancy. The optimization procedure includes partitioning the wing into three separate regions, encompassing both upper and lower skins, the spar, and ribs. Furthermore, independent optimization is applied to the upper and lower skins within each region. Significantly, there is a gradual reduction in the overall thickness and the number of composite layers from the root to the tip, corresponding to the changing bending moments experienced across the wing's span. The study also considers the presence of nine ribs with varying distances along the wing's span. To evaluate the mechanical characteristics of the laminated composites, test specimens are produced using the hand layup and vacuum bagging technique. However, in this instance, a smooth glass mold is utilized, incorporating the same carbon fiber and resin. Through experimental procedures, the mechanical properties of the composite lamina are comprehensively assessed. The outcomes of these experiments, encompassing the resulting properties, are detailed in Table 2.

Table 2. Characterized properties of the U-D composite.

E_1 (GPa)	E_2 (GPa)	G_{12} (GPa)	ν_{12}	ρ (kg/m ³)
91.52	6.54	3.6	0.27	1490
XT (MPa)	XC (MPa)	YT (MPa)	YC (MPa)	S (MPa)
1256.0	822.3	15.1	76.0	45.6

Forming a total of seven distinct laminates by dividing the upper and lower skins into three spanwise laminates and the spar into a single laminate, flexibility is provided in terms of being either unbalanced or symmetric. The optimization procedure meticulously targets specific laminates within the upper and lower skins, as well as the spar, while assigning predetermined laminates to the ribs. The primary objective is to design the wing in accordance with the specified optimization parameters (objectives, variables, constraints and load cases) and boundaries detailed in Table 3.

Table 3. Optimization parameters and boundaries.

Objectives: $f(\mathbf{x}) = \text{Wing Weight}(\mathbf{x}) - \lambda \times \text{Unit Twist Factor}(\mathbf{x})$

Variables: L_i^U [mm] (0 to 1250); L_i^L [mm] (0 to 1250); N_i^U (2 to 16); N_i^L (2 to 16); N^S (fixed at 4); θ^U [°] (-90 to 90); θ^L [°] (-90 to 90); θ^S [°] (-90 to 90); pos^R [mm] (0 to 625)

Constraints: $Buckling(\mathbf{x}) \geq 1.1$; $Static\ Strength(\mathbf{x}) \leq 0.9$; $Composite\ Failure(\mathbf{x}) \leq 0.9$; $Aeroelastic\ Instability(\mathbf{x}) \geq 75\text{m/s}$

Load Cases: *Static Load and Dynamic Load* ($U=30\text{ m/s}$, $\alpha=5^\circ$)

Gust Load (F (1 to 20); WG (0.1 to 1))

Using ANSYS Mechanical (ANSYS ACP) for structural analysis and a 3D panel aerodynamic method for static analysis, along with ZAERO's Vortex Lattice Method (VLM) code for flutter and gust analysis, is a valid and practical approach for comprehensive aeroelastic analysis of the high aspect ratio wing. The current case study involves the use of the 3D panel approach in the static aeroelastic analysis of the Structural and Composite Analysis module in the NAS² package tool [22]. Composite failure analysis is conducted by utilizing the embedded ANSYS ACP within the Structural and Composite Analysis module of the NAS² package tool. Nonlinear SHELL181 elements are utilized for all components of the composite wing, including the skins, spar, and ribs, to accurately represent the complex behavior of composite materials under aerodynamic loads. The SHELL181 element allows for geometrically nonlinear analysis, making

it suitable for simulating large deformations, buckling, and post-buckling behavior in structures subjected to various loading conditions. This analysis involves calculating the Inverse Reverse Factor (IRF). The gust response analysis and flutter analysis in the Reduced Order Aeroelastic Analysis module are performed using the VLM approach via ZAERO solver. The Optimization module utilizes the hybrid optimization approach to minimize weight and maximize the unit twist factor while taking into account aeroelastic structural and composite restrictions.

4.1 Stacking sequence of the optimized composite wing

Pursuing the selection of the optimum wing configuration that adheres to the principles of minimizing wing weight, maximizing the unit twist factor, and minimizing the IRF, the indispensable mathematical construct known as the Fitness Factor comes into play as shown in Eq. (1). The parameters are subjected to non-dimensionalization, which scales them to a defined range spanning from 0 to 1. The procedure is structured such that the ideal value for each objective and parameter (minimum wing weight, maximum unit twist factor, and minimum inverse reverse factor) is defined as 1, while the other values are assigned numerical values ranging from 0 to 1 in proportion to the ideal value of 1.

$$\frac{(C_1 \times \text{wing weight}) + (C_2 \times \text{unit twist factor}) + (C_3 \times \text{inverse reverse factor})}{C_1 + C_2 + C_3} = \text{Fitness factor} \quad (1)$$

In this methodology, weight coefficients ($C_i, i = 1,2,3$) are assigned to each objective, defining their relative significance in the design process. The Fitness Factor, applied in the current study, utilizes a weighting system attributing $C_1 = 6$, $C_2 = 2$ and $C_3 = 1$ to wing weight, unit twist factor, and inverse reverse factor, respectively. Assigning the highest weight coefficient to wing weight underscores its paramount importance in optimization. The Fitness Factor is computed for several case studies on the Pareto front (see Figure 5a), ensuring the final wing design aligns with goals and adheres to robust mathematical and engineering principles. The 1st design point, demonstrating effectiveness with a Fitness Factor of 0.83, is noteworthy (see Figure 5b).

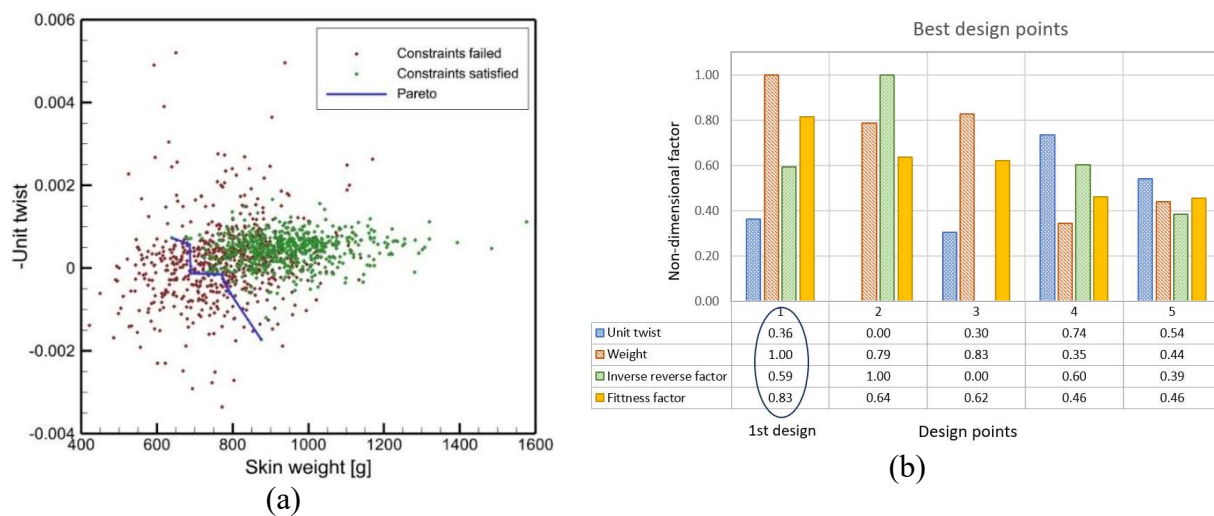


Figure 5. a) Pareto curve and b) comparing the initial five design points.

Figure 6 displays the stacking sequence of the composite wing, which shows the specific arrangement of the upper and lower skins in addition to the spar. In order to improve the flexibility of the design, the top and lower skins are divided into three separate regions, each with different lengths. These regions are shown visually in Figure 6 and are used as optimization variables to enhance the design adaptability. Each layer and region of upper and lower skins present a unique fiber angle, which emphasizes a distinguishing characteristic. The spar, ascribed to its principal function of supporting aerodynamic loads, maintains a uniform fiber angle across its entire width. The symmetric configuration of both the skins and the spar in the stacking sequence is critical for maintaining structural integrity and balance in the design. The lengths of these regions and their accompanying outcomes are displayed in Figure 6.

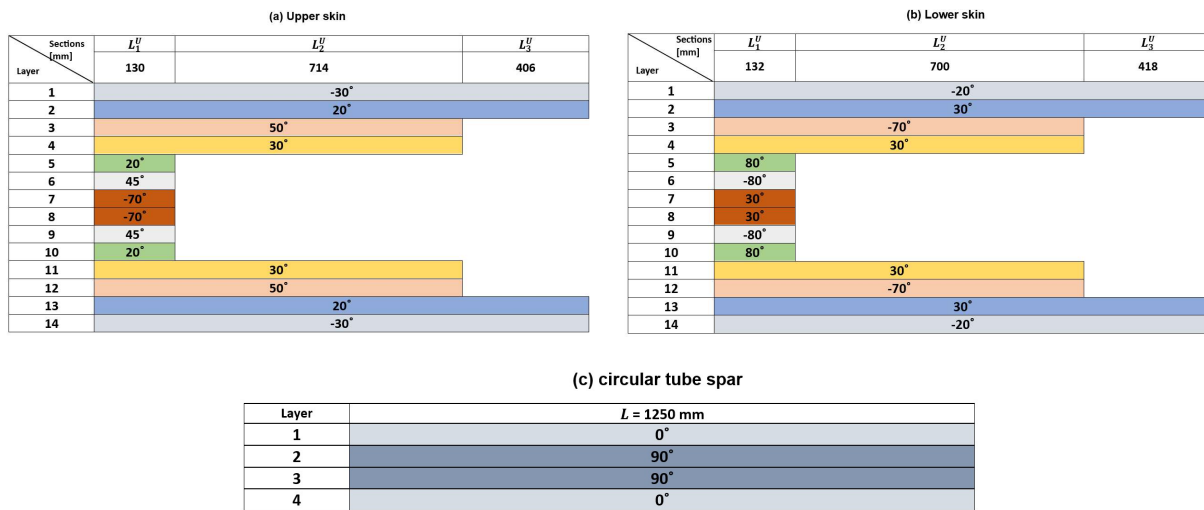


Figure 6. Arrangement of the upper and lower wing skins along with the spar in the stacking sequence.

4.2 Static flapwise deformation of the optimized wing

Comparing the static deformation of the optimized wing in flapwise direction, Figure 7 contrasts two methodologies: geometrically linear and nonlinear (assuming small and large deformations). At a flight speed of 30 m/s with $\alpha=5^\circ$, the comparison reveals a significant difference in the wing tip deflection. The nonlinear model, at $\alpha=5^\circ$, reveals a 21.1% higher deflection compared to the linear model, exposing the conservative nature of the linear assumptions.

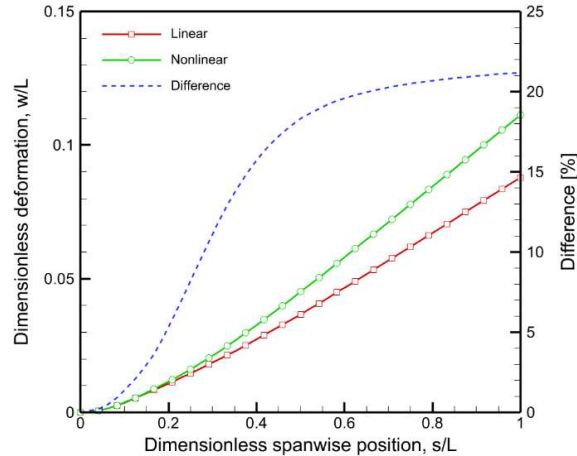


Figure 7. Comparing the vertical deformation of the optimized wing with both geometric linearity and nonlinearity for $\alpha=5^\circ$

4.3 Inverse reserve factor (IRF) and buckling distribution of the optimized wing

The reciprocal of the ratio between applied stress or load and critical stress or load, known as the IRF, serves as a key indicator of structural proximity to failure. This factor is crucial for assessing structural safety, with a lower value indicating a larger safety margin, signifying greater distance from failure. Conversely, a higher IRF suggests a smaller safety margin, signaling closer proximity to failure. Figures 8a and 8b highlight a significant difference in the inverse reserve factor between geometrically linear and nonlinear solutions. This contrast emerges when accounting for large deformations in the wing under aerodynamic loads. In the nonlinear solution, vulnerable zones in the upper and lower skins, especially the leading-edge part of the upper skin and transition areas of region 1 and 2, are prone to structural and composite failure. In linear analysis, the lower skin shows higher susceptibility to failure compared to the upper skin, while in the nonlinear solution, the upper skin exhibits higher susceptibility to failure. Statically the disparity between linear and nonlinear solutions, revealing a notable 27.53% difference for $\alpha=5^\circ$.

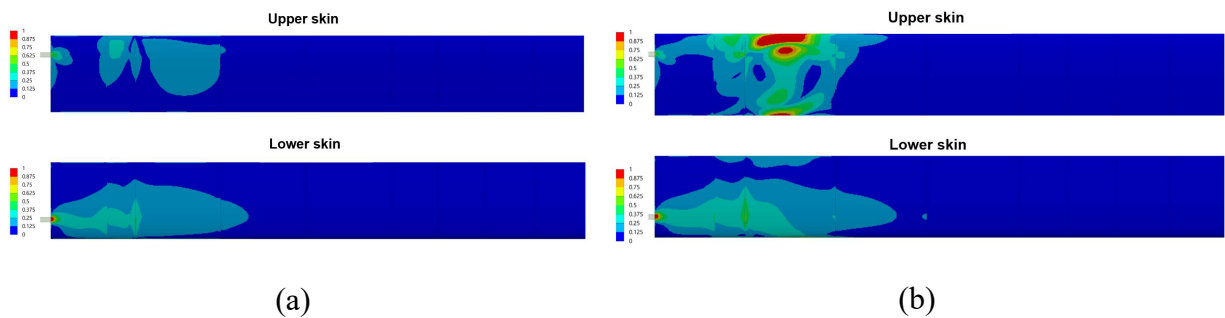


Figure 8. IRF for upper and lower skins for $\alpha=5^\circ$ a) geometrically linear and b) geometrically nonlinear solutions

4.4 Structural dynamic and gust response

Figure 9 exhibits the inherent frequencies and the accompanying patterns of motion of the optimized composite wing. The acronyms utilized in Figure 10 are "FB" for Flapwise Bending, "CB" for Chordwise Bending, and "T" for Torsion. The initial three modes consist of 1st FB, 1st CB, and 2nd FB, whereas the 4th and 5th modes correspond to the coupling modes of T and FB.

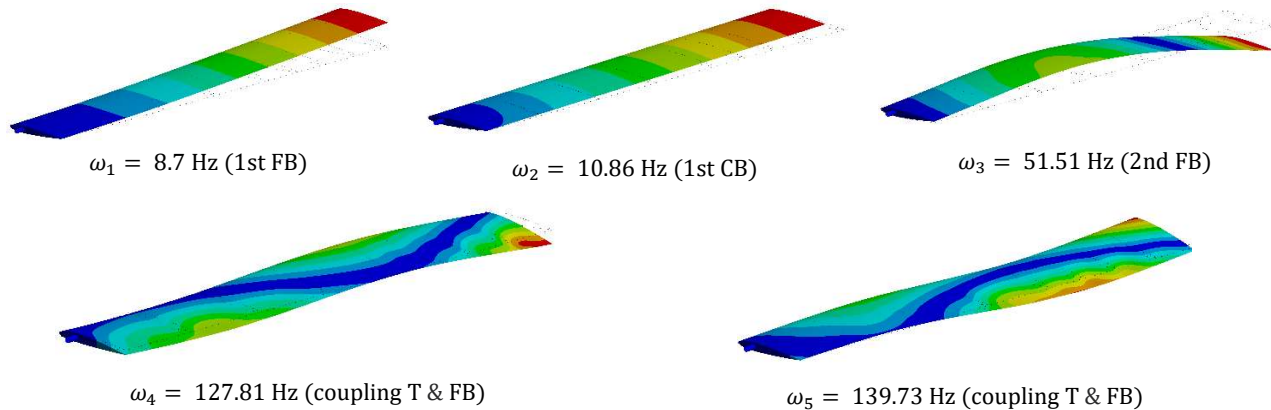


Figure 9. Natural frequencies and corresponding mode shapes of the clamped wing

Figure 10 illustrates the performance of the optimized composite wing when exposed to the 1-cosine gust model. The primary parameters under investigation for wing gust loading responses are the root bending moment and the wing tip deflection.

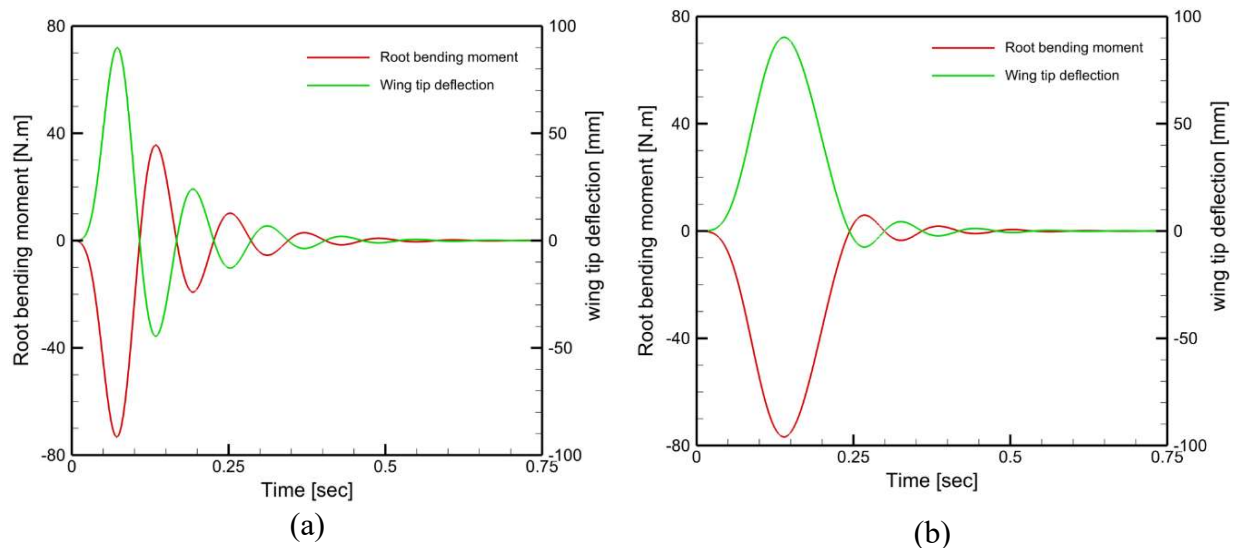


Figure 10. Gust response to 1-cosine gust with gust amplitude of $WG = 0.1$ and (a) gust frequency of 12.5 Hz and (b) gust frequency of 4 Hz.

5 CONCLUSIONS

This research introduces an aeroelastic tailored Multi-objective, Multi-disciplinary Design Optimization (MDO) approach that seamlessly integrates numerical optimization techniques. The

aim is to minimize weight and ensure structural integrity. The proposed numerical methodology, integrated within the fully automated Nonlinear Aeroelastic Simulation Software (NAS²) package, combines FEM code for simulating structural performance, an in-house ROM framework for flutter and gust analysis and Two-way coupling method for geometrically nonlinear static aeroelastic analyses, and a hybrid PSO and GA technique as an optimization method. Establishing a robust numerical approach, this integration is designed for the improved aeroelastic and structural performance of composite wings. Through this multidisciplinary approach, we emphasize the pivotal role of tailoring aeroelastic solutions in the advanced design and manufacturing of high-aspect-ratio composite wings, contributing to the continued evolution of aerospace technology.

ACKNOWLEDGMENT

This study has been supported by the Scientific and Technological Research Council of Türkiye (TÜBİTAK, Project No. 220N396 and TÜBİTAK 2219 program). The authors gratefully acknowledge the support of this study.

REFERENCES

- [1] Farsadi, T., Rahmanian, M., & Kayran, A. (2018). Geometrically nonlinear aeroelastic behavior of pretwisted composite wings modeled as thin walled beams. *Journal of Fluids and Structures*, 83, 259-292.
- [2] Farsadi, T., Rahmanian, M., & Kayran, A. (2020). Reduced order nonlinear aeroelasticity of swept composite wings using compressible indicial unsteady aerodynamics. *Journal of Fluids and Structures*, 92, 102812.
- [3] Sina, S. A., Farsadi, T., & Haddadpour, H. (2013). Aeroelastic stability and response of composite swept wings in subsonic flow using indicial aerodynamics. *Journal of Vibration and Acoustics*, 135(5), 051019. 57.
- [4] Asadi, D., Farsadi, T., & Kayran, A. (2021). Flutter optimization of a wing–engine system with passive and active control approaches. *AIAA Journal*, 59(4), 1422-1440.
- [5] Asadi, D., & Farsadi, T. (2020). Active flutter control of thin walled wing-engine system using piezoelectric actuators. *Aerospace Science and Technology*, 102, 105853.
- [6] Wunderlich, T. F. (2015). Multidisciplinary wing optimization of commercial aircraft with consideration of static aeroelasticity. *CEAS Aeronautical Journal*, 6(3), 407-427.
- [7] Zhao, W., & Kapania, R. K. (2017). Static aeroelastic optimization of aircraft wing with multiple surfaces. *In 18th AIAA/ISSMO Multidisciplinary Analysis and Optimization Conference* (p. 4320).
- [8] Dillinger, J. K. S., Klimmek, T., Abdalla, M. M., & Gürdal, Z. (2013). Stiffness optimization of composite wings with aeroelastic constraints. *Journal of Aircraft*, 50(4), 1159-1168.
- [9] Mitrotta, F. M. A., Rajpal, D., Sodja, J., & De Breuker, R. (2020). Multi-fidelity design of an aeroelastically tailored composite wing for dynamic wind-tunnel testing. *In AIAA Scitech 2020 Forum* (p. 1636).
- [10] Farsadi, T., Asadi, D., & Kurtaran, H. (2021). Fundamental frequency optimization of variable stiffness composite skew plates. *Acta Mechanica*, 232(2), 555-573.

- [11] Handojo, V., Himisch, J., Bramsiepe, K., Krüger, W. R., & Tichy, L. (2022). Potential Estimation of Load Alleviation and Future Technologies in Reducing Aircraft Structural Mass. *Aerospace*, 9(8), 412.
- [12] Farsadi, T., Rahmanian, M., & Kurtaran, H. (2021). Nonlinear lay-up optimization of variable stiffness composite skew and taper cylindrical panels in free vibration. *Composite Structures*, 262, 113629.
- [13] Wang, Y., Li, X., Wu, T., & Yin, H. (2023). Multidisciplinary Design and Optimization of Variable Camber Wing with Non-Equal Chord. *Aerospace*, 10(4), 336.
- [14] Benaouali, A., & Kachel, S. (2019). Multidisciplinary design optimization of aircraft wing using commercial software integration. *Aerospace Science and Technology*, 92, 766-776.
- [15] Silva, G. H., do Prado, A. P., Cabral, P. H., De Breuker, R., & Dillinger, J. K. (2019). Tailoring of a composite regional jet wing using the slice and swap method. *Journal of Aircraft*, 56(3), 990-1004.
- [16] Saporito, M., Da Ronch, A., Bartoli, N., & Defoort, S. (2023). Robust multidisciplinary analysis and optimization for conceptual design of flexible aircraft under dynamic aeroelastic constraints. *Aerospace Science and Technology*, 108349.
- [17] Rajpal, D., Gillebaart, E., & De Breuker, R. (2019). Preliminary aeroelastic design of composite wings subjected to critical gust loads. *Aerospace Science and Technology*, 85, 96-112.
- [18] Kilimtzidis, S., & Kostopoulos, V. (2023). Static Aeroelastic Optimization of High-Aspect-Ratio Composite Aircraft Wings via Surrogate Modeling. *Aerospace*, 10(3), 251.
- [19] Meddaikar, Y. M., Dillinger, J. K., Sodja, J., Mai, H., & De Breuker, R. (2016). Optimization, manufacturing and testing of a composite wing with maximized tip deflection. In *57th AIAA/ASCE/AHS/ASC Structures, Structural Dynamics, and Materials Conference* (p. 0489).
- [20] Krüger, W. R., Meddaikar, Y. M., Dillinger, J. K., Sodja, J., & De Breuker, R. (2022). Application of Aeroelastic Tailoring for Load Alleviation on a Flying Demonstrator Wing. *Aerospace*, 9(10), 535.
- [21] Rajpal, D., Mitrotta, F. M. A., Socci, C. A., Sodja, J., Kassapoglou, C., & De Breuker, R. (2021). Design and testing of aeroelastically tailored composite wing under fatigue and gust loading including effect of fatigue on aeroelastic performance. *Composite Structures*, 275, 114373.
- [22] Farsadi, T., Ahmadi, M., Sahin, M., Haddad Khodaparast, H., Kayran, A., & Friswell, M. I. (2024). High Aspect Ratio Composite Wings: Geometrically Nonlinear Aeroelasticity, Multi-Disciplinary Design Optimization, Manufacturing, and Experimental Testing. *Aerospace*, 11(3), 193.
- [23] Ahmadi, M., Farsadi, T., & Khodaparast, H. H. (2024). Enhancing Gust Load Alleviation Performance in an Optimized Composite Wing using Passive Wingtip Devices: Folding and Twist Approaches. *Aerospace Science and Technology*, 109023.
- [24] Ahmadi, M., & Farsadi, T. (2024). Multidisciplinary optimization of high aspect ratio composite wings with geometrical nonlinearity and aeroelastic tailoring. *Aerospace Science and Technology*, 145, 108849.

[25] Rafiee, R., Farsadi, T., Tehrani, M. A., & Sharifi, P. (2023). Linkage Learning Optimization of Aeroelastic and Structural Behavior of Composite Wings. *International Journal of Aeronautical and Space Sciences*, 24(5), 1187-1198.

COPYRIGHT STATEMENT

The authors confirm that they, and/or their company or organization, hold copyright on all of the original material included in this paper. The authors also confirm that they have obtained permission from the copyright holder of any third-party material included in this paper to publish it as part of their paper. The authors confirm that they give permission, or have obtained permission from the copyright holder of this paper, for the publication and public distribution of this paper as part of the IFASD 2024 proceedings or as individual off-prints from the proceedings.